

Scaling and fractality in fatigue resistance: Specimensize effects on Wöhler's curve and fatigue limit

*Original*

Scaling and fractality in fatigue resistance: Specimensize effects on Wöhler's curve and fatigue limit / Carpinteri, Alberto; Montagnoli, Francesco; Invernizzi, Stefano. - In: FATIGUE & FRACTURE OF ENGINEERING MATERIALS & STRUCTURES. - ISSN 8756-758X. - 43:8(2020), pp. 1869-1879. [10.1111/ffe.13242]

*Availability:*

This version is available at: 11583/2838356 since: 2020-07-05T13:12:31Z

*Publisher:*

Wiley

*Published*

DOI:10.1111/ffe.13242

*Terms of use:*

This article is made available under terms and conditions as specified in the corresponding bibliographic description in the repository

*Publisher copyright*

Wiley postprint/Author's Accepted Manuscript

This is the peer reviewed version of the above quoted article, which has been published in final form at <http://dx.doi.org/10.1111/ffe.13242>. This article may be used for non-commercial purposes in accordance with Wiley Terms and Conditions for Use of Self-Archived Versions.

(Article begins on next page)

**Scaling and fractality in fatigue resistance:**  
**Specimen-size effects on Wöhler's curve and fatigue limit**

Alberto Carpinteri<sup>a</sup>, Francesco Montagnoli<sup>\*a</sup>, Stefano Invernizzi<sup>a</sup>

<sup>a</sup>Politecnico di Torino, Department of Structural, Geotechnical and Building Engineering, Corso Duca degli Abruzzi 24,  
10129 Torino, Italy

\* Corresponding Author. Tel.: +39 011 090 4807; fax: +39 011 090 4899. E-mail address:  
francesco.montagnoli@polito.it

**Abstract**

The present contribution investigates size effects on Wöhler's curve in accordance with dimensional analysis and intermediate asymptotics theory. These approaches provide a generalized equation able to interpret the specimen-size effects on Wöhler's curve. Subsequently, using a different approach based on lacunar fractality concepts, analogous scaling laws are found for the coordinates of the limit-points of Wöhler's curve, so that a theoretical explanation is provided to the decrement in fatigue resistance by increasing the specimen size. Eventually, the proposed models are compared to experimental data available in the Literature, which seem to confirm the advantage of applying Fractal Geometry to the problem.

**Keywords:** Wöhler's curve, Dimensional analysis, Intermediate asymptotics, Fractal geometry, Size-scale effects, Fatigue limit

**Nomenclature**

$\Delta\sigma$  stress range

$\Delta\sigma^*$  fractal stress range

$\Delta\sigma_0$	Basquin's parameter
$\Delta\sigma_{cr}$	critical stress range
$\Delta\sigma_{cr}^*$	fractal critical stress range
$\Delta\sigma_{cr}^\infty$	asymptotic value of the critical stress range
$\Delta\sigma_{fl}$	fatigue limit
$\Delta\sigma_{fl}^*$	fractal fatigue limit
$\Delta\sigma_{fl}^\infty$	asymptotic value of the fatigue limit
$\sigma_u$	ultimate tensile strength
$\sigma_u^*$	fractal ultimate tensile strength
$\sigma_u^\infty$	asymptotic value of the ultimate tensile strength
<i>area</i>	orthogonally projected area of the defect with respect to the applied stress range
<i>b</i>	specimen size
$d_\sigma$	dimensional decrement of ligament area
<i>HV</i>	Vickers hardness
$K_{IC}$	fracture toughness
$l_{ch}$	characteristic material length
<i>N</i>	number of cycles
$N_{cr}$	number of cycles below which tensile resistance is not decreasing
$N_{fl}$	number of cycles beyond which fatigue resistance is not decreasing
<i>n</i>	exponent of Basquin's law
<i>R</i>	loading ratio

## 1 Introduction

Fatigue failure represents one of the most common causes of collapse of industrial and civil structures, where more than 90% of failures can be considered as the result of this phenomenon. The first research on the fatigue problem was carried out by Wöhler [1], who performed a series of experimental tests on unnotched steel specimens subjected to cyclic loading. This *modus operandi* permitted to determine the number of cycles to failure as a function of the applied stress range,  $\Delta\sigma$ , which, through the best fitting of the experimental data, allowed to obtain the so-called Wöhler's curve.

In this empirical S-N curve, it is possible to distinguish three different regions. In the first one, the failure occurs for low numbers of cycles with considerable plastic deformations, and the Coffin-Manson relationship holds. On the other hand, in the high cycle fatigue region, plastic deformations become negligible and a power-law approximation can be used, i.e. the so-called Basquin's law [2]:

$$\Delta\sigma = \frac{\Delta\sigma_0}{N^{1/n}} \quad (1)$$

The latter represents the equation of a straight line in the bi-logarithmic diagram, where  $1/n$  is the slope, whereas  $\Delta\sigma_0$  is the intercept. The transition between the LCF regime and the Basquin's regime is defined by the limit-point A, which is the intersection between the horizontal line of stress range at static failure  $\Delta\sigma_{cr}$ , and the Basquin's straight line in the bi-logarithmic diagram. The x-coordinate of the point A is equal to  $N_{cr}$ , which ranges between  $10^3$ - $10^4$  cycles [3]. Eventually, the third region corresponds to the so-called infinite-life region, where a constant fatigue limit,  $\Delta\sigma_{fl}$ , is attained. The existence and value of  $\Delta\sigma_{fl}$  is still debated for different materials and applications. The transition between Basquin's regime and infinite-life region is defined by point B. The x-coordinate of point B, ( $N_{fl}$  in Fig.1), is conventionally assumed equal to  $10^7$  cycles.

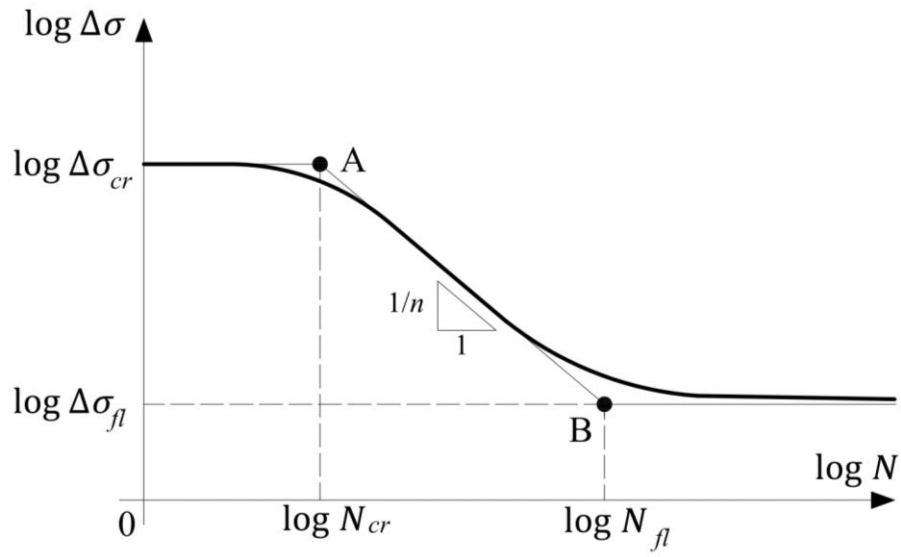


Figure 1: Wöhler's curve

According to Harte [4], the first experimental detection of the size effects in fatigue dates back to 1930. The first quantitative interpretation was obtained a decade later on the basis of statistical theories [5]. In the 1980's some researchers provided alternative formulations exploiting intermediate asymptotics theory [6]. In addition, Murakami determined experimentally a relationship between the fatigue limit and the defect of maximum size, the so-called  $\sqrt{area}$  model [7-9]:

$$\Delta\sigma_{fl} = \frac{1.56(HV + 120)}{(\sqrt{area})^{1/6}} \quad (2)$$

where  $\sqrt{area}$  is the square root of the area of the defect of maximum size projected onto a plane orthogonal to the maximum tensile stress, and is measured in  $\mu\text{m}$ ,  $HV$  being the Vickers hardness of the material. The maximum size of the inclusion, embedded in the risk volume, can be estimated by extreme value statistics [10], once that the distribution of defects in the standard inspection volume has been experimentally assessed. The risk volume is usually defined as the region where the stress is higher than the 90% of the peak value.

Murakami et al. noted also that, when a specimen fails in ultralong life regime, the fatigue fracture does not originate from the surface but near an internal inclusion, which can be clearly identified by fractography, thanks to the so-called fish-eye morphology, and by the surrounding Optically Dark Area [11, 12].

Since the development of ultrasonic fatigue testing machines, working at a very high frequency and allowing for very high number of cycles tests in a relatively short time, the interest of the scientific community about the size effects on the fatigue limit has increased [13, 14]. Furuya [15] performed ultrasonic fatigue tests on a high-strength steel and assessed the size-effect on the fatigue limit according to Eq.(2), which states that the larger the risk volume, the lower the fatigue limit.

Paolino et al. [16, 17], and Tridello et al. [18-20], in order to investigate the statistical size effect on the fatigue strength, designed an innovative specimen shape with Gaussian profile, which can be used to enlarge the risk volume of the specimen. Therefore, they were able to test a high strength steel, AISI H13, and to analyse results from a wide range of different risk volumes.

Decades ago, the concept of fractality was exploited by A. Carpinteri [21] to explain the size effect on LEFM parameters. In this framework, the material disorder due to the presence of a distribution of flaws, inclusions, and micro-cracks, is accounted for adopting a fractal, rather than Euclidean, geometrical model. In this way, the statistical population of defects is replaced by a fractal medium, which is populated of defects and lacunarities at each scale of observation. Following this approach, An. Carpinteri et al. [22] provided an expression for the experimentally observed specimen-size effects on Basquin's law.

Purpose of the present paper is to apply the concepts of dimensional analysis and incomplete self-similarity to Wöhler's curve, so that the different functional dependencies of the fatigue life can be considered through a power-law expression. Subsequently, by modelling the reacting section as a lacunar fractal domain with a non-integer dimension, which is lower than 2, it is possible to confirm the specimen-size dependence of Wöhler's curve, which is experimentally found in the Literature. Moreover, in order to model the variation of the fatigue limit over a wide size range, a Multi-Fractal Scaling Law (MFSL) is proposed for this parameter. Eventually, the proposed models are compared to experimental data available in the Literature, which seem to confirm the advantage of applying a fractal model to the specimen-size effect on Wöhler's curve.

## 2 Intermediate Asymptotics applied to Wöhler's curve

In accordance with dimensional analysis, the following functional dependence can be considered for Wöhler's curve [23, 24]:

$$N = \Pi(\Delta\sigma, 1 - R; \sigma_u, K_{IC}, \Delta\sigma_{fl}; b) \quad (3)$$

where we assume that the number of cycles to failure,  $N$ , is the parameter to be determined. The latter is a function of three different categories of variables:

1. parameters that take into account the testing conditions, i.e. the stress range,  $\Delta\sigma$ , and the loading ratio,  $R$ ;
2. parameters that take into account the static and cyclic material properties, such as the ultimate tensile stress,  $\sigma_u$ , the fracture toughness,  $K_{IC}$ , and the fatigue limit,  $\Delta\sigma_{fl}$ ;
3. the geometric parameter, i.e. the characteristic specimen size  $b$ .

Actually, we are neglecting the dependence on the time, i.e. on the frequency. The dimensions of the parameters in Eq.(3) are expressed in the Length-Force-Time class:

$$N = 1 - R = [-], K_{IC} = [F][L]^{-3/2}, \Delta\sigma = \Delta\sigma_{fl} = \sigma_u = [F][L]^{-2}, b = [L]$$

From dimensional analysis [25], since only two quantities are dimensionally independent, the number of parameters involved in the problem could be reduced from six to four, so that Eq.(3) becomes:

$$N = \bar{\Pi}\left(\frac{\Delta\sigma}{\sigma_u}, 1 - R; \frac{\Delta\sigma_{fl}}{\sigma_u}; \frac{\sigma_u^2}{K_{IC}^2} b\right) \quad (4)$$

where the following dimensionless parameters have been introduced:

$$\Pi_1 = \frac{\Delta\sigma}{\sigma_u}; \Pi_2 = 1 - R; \Pi_3 = \frac{\Delta\sigma_{fl}}{\sigma_u}; \Pi_4 = \left(\frac{\sigma_u}{K_{IC}}\right)^2 b$$

Let us observe that  $\Pi_4$  is responsible for the specimen-size dependence of the fatigue behaviour. In fact, the latter is equal to the inverse of the square of the brittleness number,  $s$  [26].

The intermediate asymptotics theory allows us to further reduce the number of quantities involved in Eq.(5) [27-30]. To this aim, let us assume an incomplete self-similarity in the dimensionless parameters  $\Pi_i$ , so that a power-law dependence of the number of cycles,  $N$ , on  $\Pi_i$  can be obtained:

$$N = \left(\frac{\Delta\sigma}{\sigma_u}\right)^{\alpha_1} (1 - R)^{\alpha_2} \left(\frac{\Delta\sigma_{fl}}{\sigma_u}\right)^{\alpha_3} \left(\frac{\sigma_u^2}{K_{IC}^2} b\right)^{\alpha_4} \quad (5)$$

Therefore, in Eq.(5) the main functional dependencies of  $N$  have been considered, so that a generalized Wöhler's relationship is obtained. For instance, the S-N curve can be approximated by the Basquin power-law for high-cycle fatigue:

$$N_{cr} \times \Delta\sigma_{cr}^n = N \times \Delta\sigma^n = 1 \times \Delta\sigma_0^n = \text{constant} \quad (6)$$

Hence, by matching the left-hand side of Eq.(6) with the right-hand side, we can write the following power-law:

$$N = N_{cr} \left(\frac{\Delta\sigma_{cr}}{\Delta\sigma}\right)^n \quad (7)$$

Furthermore, considering the relationship between ultimate tensile strength and loading ratio:

$$\Delta\sigma_{cr} = (1 - R) \sigma_u \quad (8)$$

we obtain the expression that relates the number of cycles to failure to the stress range:

$$N \propto \frac{(1 - R)^n \sigma_u^n}{\Delta\sigma^n} \quad (9)$$

Comparing the generalized expression of the S-N curve in Eq.(5) with the empirical one in Eq.(9), a perfect correspondence between them exists if:

$$\alpha_1 = -n, \quad \alpha_2 = -n \quad (10a)$$

$$\alpha_3 = \alpha_4 = 0 \quad (10b)$$

which implies an incomplete self-similarity in  $\Pi_1$  and  $\Pi_2$ , and a complete self-similarity in  $\Pi_3$  and  $\Pi_4$ , i.e. Basquin's law does not take into account the size effects.

### 3 Some remarks on the lacunar fractality and multi-fractality

In the last few decades, it has been widely recognised that the nominal tensile strength is not a material constant, but rather it depends on the structural size. As a matter of fact, the ultimate strength of a material decreases with the specimen size and this trend is more pronounced for more disordered materials [21]. In other words, the reacting section or ligament of a disordered material can be modelled as a fractal set, where its non-integer dimension lower than 2 is the way to quantify the disorder itself [31]. Thus, supposing that the total force is transmitted through a lacunar fractal ligament of dimension  $\alpha = 2 - d_\sigma$ , with  $1 \leq \alpha \leq 2$ , the following scaling law for nominal tensile strength can be proved [32-35]:

$$\sigma_u = \sigma_u^* b^{-d_\sigma} \quad (11)$$

where  $\sigma_u^*$  is the scale-invariant tensile strength with non-integer physical dimensions  $[F][L]^{-(2-d_\sigma)}$ , whereas  $d_\sigma$  is the dimensional decrement of the ligament due to the presence of cracks and voids distributions [21, 32]. Eventually, Eq.(11) can be written as:

$$\log \sigma_u = \log \sigma_u^* - d_\sigma \log b \quad (12)$$

which represents the equation of a straight line in the bi-logarithmic diagram. Notice that the fractal dimension in Eq.(11) is constant, so that we should talk about fractal scaling law. On the other hand, if we consider specimens with a very wide size range, the experimental results point out that a fractal scaling approach is valid only within a limited scale range, such that the fractal dimension can be really considered constant. This implies that, as the specimen size increases, the concept of geometrical multi-fractality should be put forward, i.e. a change of  $d_\sigma$  with the scale of observation [36-38].

This can be explained by recalling that the microstructure of a disordered material remains the same independently of the scale of observation. As a result, the influence of disorder on mechanical properties depends on the ratio between a characteristic material length,  $l_{ch}$ , and the characteristic size of the specimen,  $b$ . Hence, the effect of disordered nature on the mechanical parameters of the material turns out gradually less important for larger scales of observation and, eventually, the fractality vanishes for  $b$  tending to infinity.

This transition from a disordered regime for smaller scales, where the fractal scaling exponent is equal to 1/2 due to a self-similar distribution of cracks, to an ordered regime for larger scales can, therefore, be considered for any mechanical quantity [36]. The analytical expression of the Multi-Fractal Scaling Law (MFSL) for tensile strength is the following (Fig.2) [39-41]:

$$\sigma_u(b) = \sigma_u^\infty \left(1 + \frac{l_{ch}}{b}\right)^{1/2} \quad (13)$$

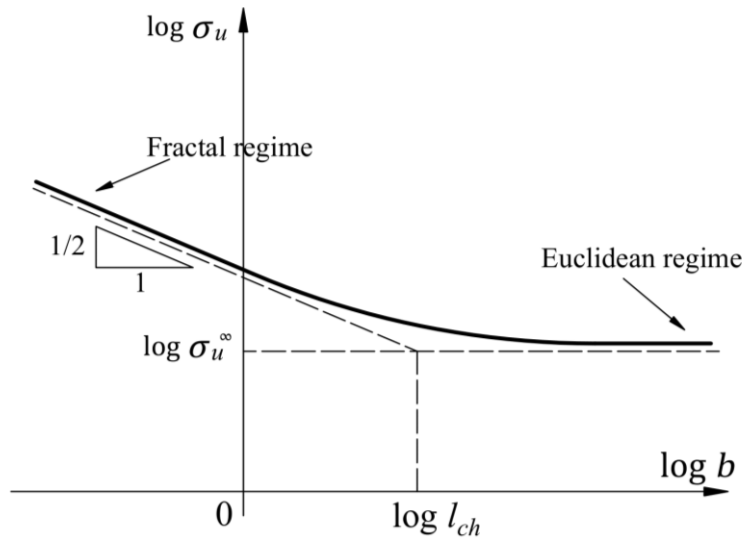


Figure 2: Size effect on ultimate tensile strength

This scaling law represents a two-parameter best-fitting, where the asymptotic value of the ultimate strength,  $\sigma_u^\infty$ , corresponding to its lowest value, is reached only in the limit case of infinite specimen sizes. Furthermore, the variable influence of disorder on tensile strength is represented by the dimensionless term within round brackets, which depends on the characteristic length  $l_{ch}$ . In other words, in the bi-logarithmic diagram, the transition from the fractal regime to the Euclidian one is represented by the point of asymptotes' intersection of abscissa  $\log l_{ch}$ , which is a function of the microstructure of the material [42-44]. The characteristic material length  $l_{ch}$  is a material property that can be proportional to the average defect size, or to the grain size, or to the inclusion size, depending on the mechanism responsible for fracture nucleation.

#### 4 Fractal and multi-fractal approach to Wöhler's curve

As mentioned in the Introduction, experimental evidences have pointed out a size effect on fatigue strength, which generally decreases with the specimen size. Although in the Literature have been proposed different interpretations able to give an explanation to the problem, such as Murakami's model, these consider only the maximum size defect, so neglecting the microstructural disorder of

the material. Thus, by exploiting the renormalized quantities related to a lacunar fractal cross-section, the following scaling law for the stress range can be written [22, 45]:

$$\Delta\sigma = \Delta\sigma^* b^{-d_\sigma} \quad (14)$$

where the fractal stress range  $\Delta\sigma^*$ , with physical dimensions given by  $[F][L]^{-(2-d_\sigma)}$ , is considered invariant with respect to the scale of observation. Furthermore, since  $0 \leq d_\sigma \leq 1$ , Eq.(14) predicts a decrement in the number of cycles to failure with the specimen size. On the other hand, considering the stress range as a function of  $N$ , Eq.(14) predicts a decrease in  $\Delta\sigma$  with the specimen size,  $N$  being the same. Thus, Eq.(14) allows us to demonstrate that the fatigue strength undergoes size effects. It is worth noting that the assumption of the ligament lacunar fractality can be comprised in the intermediate asymptotics framework, when the dimensionless parameter  $b \sigma_u^2 / K_{IC}^2$  is provided with the non-integer exponent  $\alpha_4 = -d_\sigma n$ .

Similarly, the fractal approach can be used to explain the specimen-size effects on fatigue limit. In fact, since the fatigue limit is experimentally determined for a conventional very high number of cycles, Eq.(14) can be evaluated in correspondence to the right knee-point of Wöhler's curve, i.e.  $N = N_{fl}$ , so that the following scaling law for the fatigue limit is obtained:

$$\Delta\sigma_{fl} = \Delta\sigma_{fl}^* b^{-d_\sigma} \quad (15)$$

where  $\Delta\sigma_{fl}^*$  is the fractal fatigue limit, which is a material property with anomalous physical dimensions. Hence, Eq.(16) provides the specimen-size effect on the fatigue limit. Indeed, in agreement with the concept of lacunar fractal set, we obtain a negative slope for the fatigue limit by varying the specimen size, i.e. Eq.(16) provides a decrement in  $\Delta\sigma_{fl}$  with the specimen size. Eventually, Eq.(29.b) can be written in the following form:

$$\log \Delta\sigma_{fl} = \log \Delta\sigma_{fl}^* - d_\sigma \log b \quad (16)$$

which represents the equation of a straight line with slope equal to  $-d_\sigma$  in a bi-logarithmic diagram. Analogously, it is possible to define the specimen-size effect on the left knee-point of Wöhler's curve,

i.e. for  $N = N_{cr}$ . Thus, evaluating Eq.(15) in correspondence of it, we obtain the following scaling law for the ordinate of the critical point:

$$\Delta\sigma_{cr} = \Delta\sigma_{cr}^* b^{-d_\sigma} = (1 - R) \sigma_u^* b^{-d_\sigma} \quad (17)$$

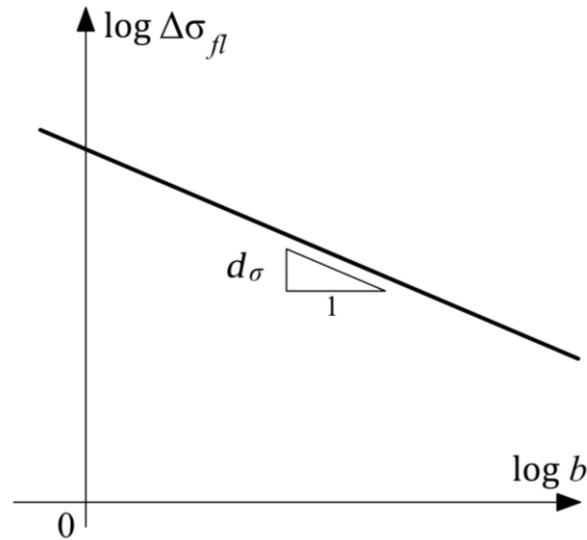


Figure 3: Specimen-size effects on fatigue limit in a bi-logarithmic diagram

Thus, Eqns. (15) and (17) yield a vertical downward translation of Wöhler's curve increasing the specimen size, i.e. the larger the specimen dimension, the lower the fatigue strength. Thus, it is worth to note that, being  $N_{cr}$  and  $N_{fl}$  dimensionless parameters, only the vertical translation is expected (Fig.4), excluding the horizontal one [46]. On the other hand, substituting the nominal stress range with the corresponding fractal parameter, a fractal coordinate system is obtained and a collapse of the set of specimen-size dependent Wöhler's curves onto a single specimen-size independent Wöhler's curve is expected (Fig.5).

Moreover, notice that, for  $d_\sigma \rightarrow 1/2$ , we obtain  $\Delta\sigma_{fl} \propto b^{-1/2}$ , so that the fractal fatigue limit assumes the physical dimensions of a stress-intensity factor, i.e.  $[F][L]^{-3/2}$ . This observation implies that a value higher than 1/2 is not possible. In fact, this condition is obtained assuming a self-similar statistical size distribution such that the defect of maximum size is proportional to the structural size. As a result, this statement implies that the defect size distribution of self-similarity corresponds to the condition of maximum disorder. Hence, since the assumption of a self-similar statistical size

distribution implies a value of the scaling exponent of strength vs. structural size equal to 1/2, it follows that the maximum possible value for  $d_\sigma$  is 1/2 [32].

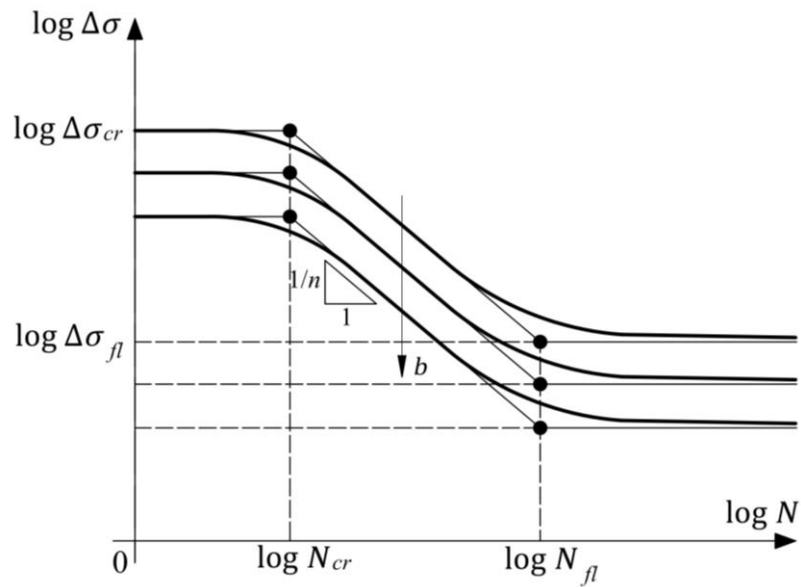


Figure 4: Specimen-size effects on Wöhler's curve

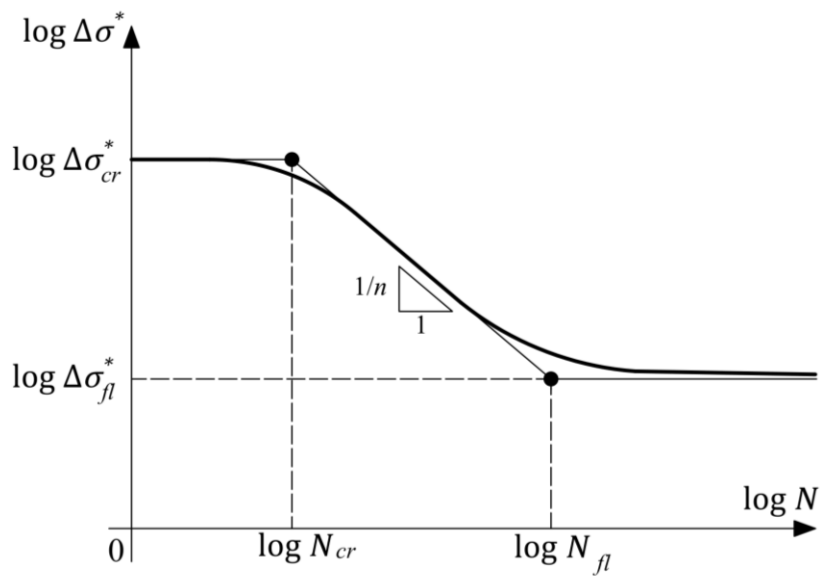


Figure 5: Fractal (specimen-size independent) Wöhler's curve

The next step concerns the introduction of the concept of self-affinity. In fact, although the decrease in fatigue limit by increasing the structural size can be obtained considering just the fractal

approach, a Multi-Fractal Scaling Law for the fatigue limit should be put forward to capture the transition from the fractal regime to the Euclidian one:

$$\Delta\sigma_{fl} = \Delta\sigma_{fl}^{\infty} \left(1 + \frac{l_{ch}}{b}\right)^{1/2} \quad (18)$$

Thus, since for very large structural sizes a transition from disorder to the Euclidian order is expected, the fractal decrement,  $d_{\sigma}$ , tends to zero. Consequently, the specimen-size dependence of fatigue limit disappears and we obtain its asymptotic value,  $\Delta\sigma_{fl}^{\infty}$ , which can be considered as a material constant. *Vice-versa*, for very small specimens, the influence of the material disorder becomes progressively more important and the fatigue limit increases as the specimen size decreases (see Fig.6). In other words, Eq.(18) provides a decrement in the fatigue limit with the specimen size according to the assumption of a lacunar fractal ligament.

The exponent of the term within round brackets represents the slope of the oblique asymptote in the bi-logarithmic diagram  $\Delta\sigma_{fl}$  vs.  $b$ , which is always lower than 1/2, as above mentioned. Furthermore, according to Eq.(17), a Multi-Fractal Scaling Law for  $\Delta\sigma_{cr}$  can be put forward to capture the transition from the fractal regime to the Euclidian one:

$$\Delta\sigma_{cr} = \Delta\sigma_{cr}^{\infty} \left(1 + \frac{l_{ch}}{b}\right)^{1/2} \quad (19)$$

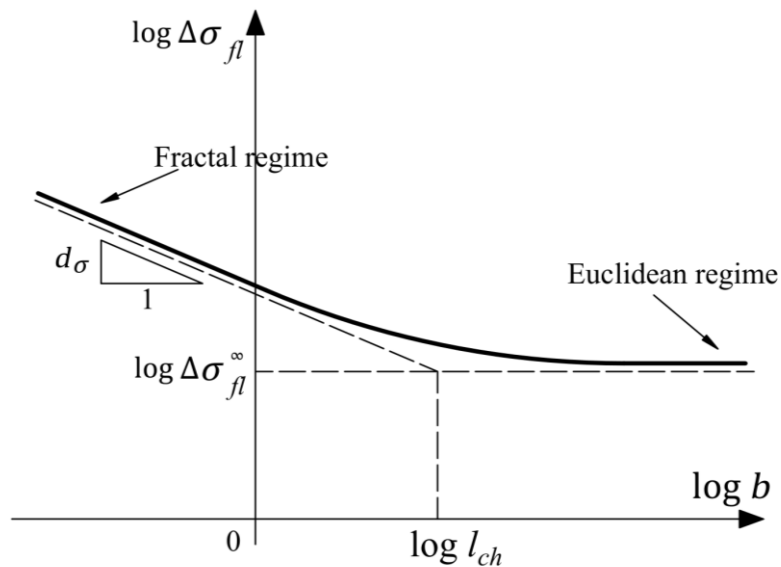


Figure 6: Multi-Fractal Scaling Law for fatigue limit

where  $\Delta\sigma_{cr}^{\infty}$  is the lowest value of  $\Delta\sigma_{cr}$ , which is reached for very large specimen sizes. Thus, since for  $b \rightarrow +\infty$  the specimen-size dependence disappears,  $\Delta\sigma_{cr}^{\infty}$  represents a material constant.

## 5 Experimental assessment of the scaling law for fatigue limit

In this section, some experimental results on aluminium alloy flat hourglass samples [47] are considered, although geometrical self-similarity of the specimens should be required for proper comparison among specimens with the same stress concentration. Different Wöhler's curves in the power-law regime are obtained for different specimen sizes, as shown in Fig.7. When the experimental results are reported in the fractal Wöhler's diagram, they collapse onto a single straight line in the power-law regime, independently of the specimen size. The renormalization of the Wöhler's diagram yields to a scale-invariant curve.

Best-fitting of experimental data, in order to collapse them onto a single curve, provides the dimensional decrement  $d_{\sigma}$ , which is equal to 0.13 in the case of the data collected in [47]. Eventually, the fractal stress-range will show the anomalous physical dimensions  $[F][L]^{-1.87}$  (see Fig.8).

Xue et al. [48] performed fatigue tests on Al-Si-Cu cast alloy specimens beyond  $10^9$  cycles with an ultrasonic fatigue testing machine operating at 20 kHz and  $R = -1$ . They considered hourglass specimens with 3 and 6 mm in diameter at the middle cross-section. The experimental data show that, for a certain number of cycles, the larger the diameter of the ligament, the lower the fatigue strength. As a consequence, in the Wöhler's diagram of Fig.9, two different curves are obtained depending on the specimen-size. On the contrary, if the fractal Wöhler's diagram of Fig.10 is adopted, all the data collapse onto a single straight line. The physical dimensions of the fractal stress range  $\Delta\sigma^*$ , equal to  $[F][L]^{-1.81}$ , are obtained by best-fitting of experimental data.

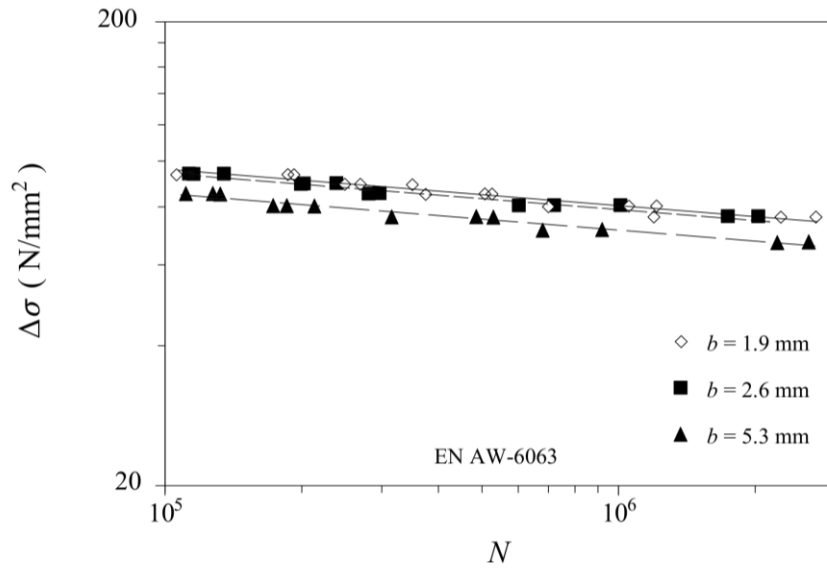


Figure 7: Experimental specimen-size dependent Wöhler's curves in the power-law regime for EN AW-6063 [47]

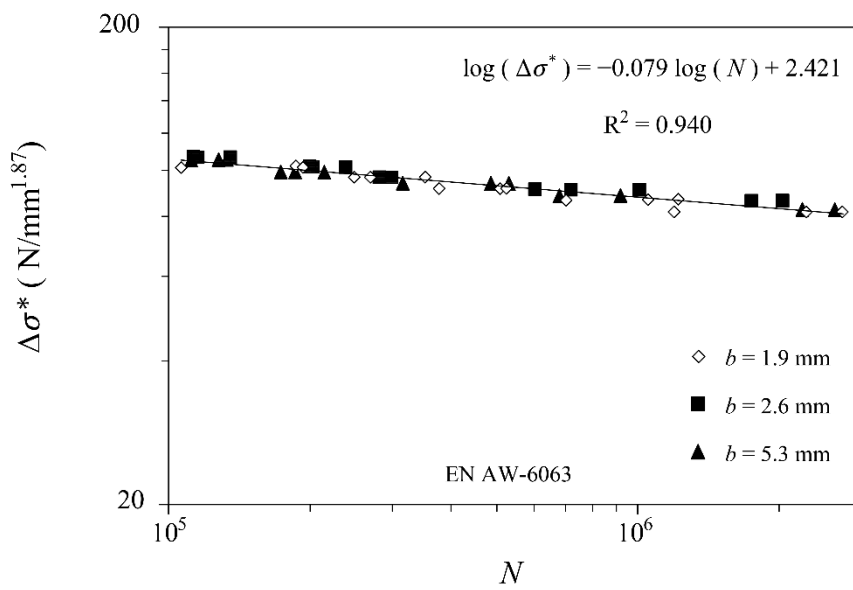


Figure 8: Experimental fractal Wöhler's curve in the power-law regime for EN AW-6063

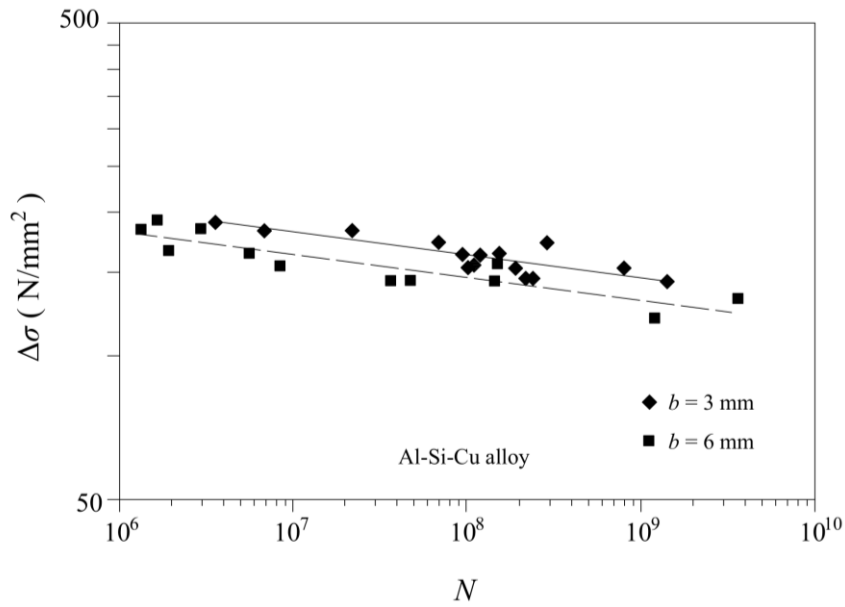


Figure 9: Experimental specimen-size dependent Wöhler's curves for Al-Si-Cu alloy [48]

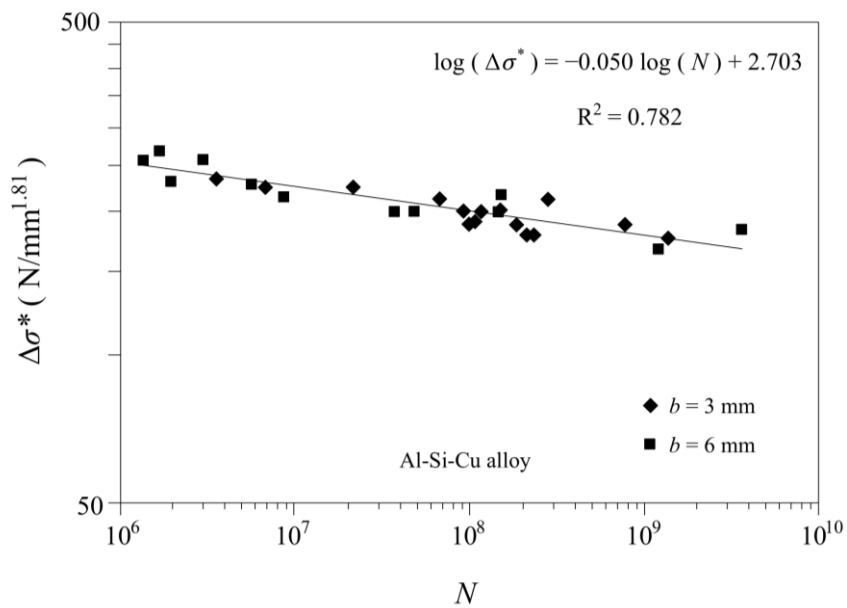


Figure 10: Experimental fractal Wöhler's curve for Al-Si-Cu alloy

In addition, in the present section the experimental data available in the Literature are fitted with Eq.(16).

Hatanaka et al. performed a set of fatigue tests to investigate the specimen-size effects on Wöhler's

curve [49]. Considering two different materials and dog-bone specimens of 8, 20, 30, and 40 mm of diameter, tests were carried out through a rotating bending machine. More specifically, the two materials used are a cast steel, JIS SCMn 2A, and a forged steel, JIS SF 50. From the test results and for both the materials, it was highlighted a decrease in the fatigue strength with the specimen size. In particular, it was observed that, in accordance with Fractal Geometry, the decrement in fatigue strength was more pronounced for the material with a less homogenous microstructure, i.e. JIS SCMn 2A.

Thus, by focusing our attention on the fatigue limit, a linear regression provides the best-fitting parameters entering Eq.(16) for the two steel alloys. Considering SF50 steel, we obtain the following equation for the fatigue limit:

$$\log \Delta\sigma_{fl} = -0.08 \log b + 2.74 \quad (20)$$

which implies that the fractal dimension decrement is equal to 0.08, thus revealing a dimension of material ligament equal to 1.92, whereas the fractal fatigue limit, which represents the true material constant, is  $279 \text{ N mm}^{-1.92}$  (see Fig.11). On the other hand, considering SCMn 2A steel, we have the following expression for the fatigue limit:

$$\log \Delta\sigma_{fl} = -0.16 \log b + 2.80 \quad (21)$$

which provides a value of the fractal dimension decrement equal to 0.16, whereas the fractal fatigue limit is  $318 \text{ N mm}^{-1.84}$  (Fig.12).

Notice that the obtained values for the fractal decrement  $d_\sigma$  are consistent. The more ordered the material, the closer the material ligament to a two-dimensional Euclidian surface. In fact, for the SF50 steel, which is the more ordered material, the dimensional decrement of the fractal domain is smaller than that obtained for SCMn 2A [50]. Eventually, it is interesting to point out that the values obtained are always lower than 1/2, in accordance with the hypothesis of statistical crack-size distribution of self-similarity [51].

As a third example, we consider the experiments carried out by Furuya on specimens made up of high-strength steel, i.e. JIS-SCM440 low-alloy steel, by means of an ultrasonic fatigue testing machine [52]. The experimental evidence shows that the fatigue failure, for this kind of steels, is

mainly caused by fish-eye fracture, i.e. an internal penny-shaped crack which is originated mostly from an inclusion [20].

These ultrasonic fatigue tests were conducted at 20 kHz, with a stress ratio  $R = -1$ . Furthermore, these tests were carried out using a dog-bone specimen of 8 mm in diameter and hourglass-shaped specimens of 7 mm and 3 mm in diameter.

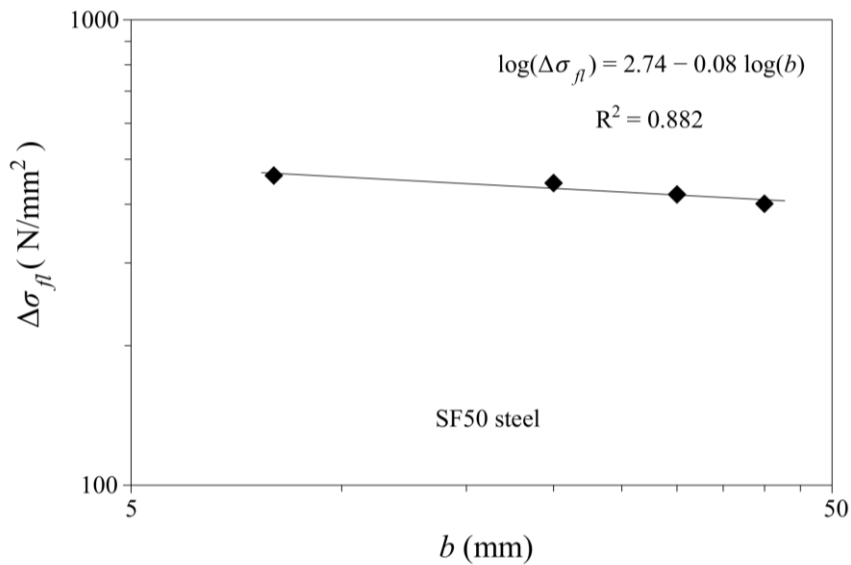


Figure 11: Experimental assessment of fatigue limit for SF50 steel [49]

As in the previous case, a linear regression permits us to obtain the following relationship for the fatigue limit:

$$\log \Delta\sigma_{f_l} = -0.16 \log b + 3.26 \quad (22)$$

which provides the values of the best-fitting parameters. Thus, considering Eq.(22), a value of the fractal dimension decrement equal to 0.16 is expected, whereas the fractal fatigue limit is  $1820 \text{ N mm}^{-1.84}$  (Fig.13).

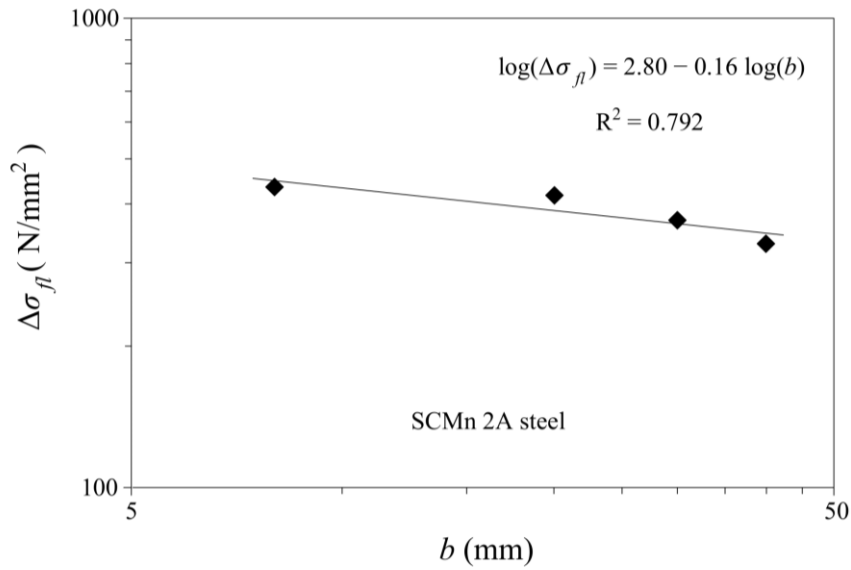


Figure 12: Experimental assessment of fatigue limit for SCMn 2A steel [49]

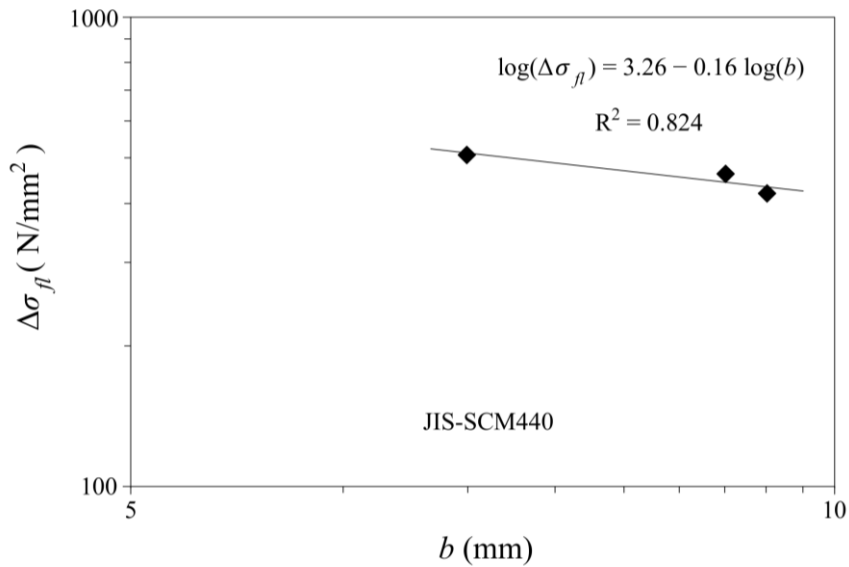


Figure 13: Experimental assessment of fatigue limit for JIS-SCM440 low-alloy steel [52]

In addition, the experimental data by Pegues et al. [53] on additively manufactured Ti-6Al-4V titanium alloy samples are analysed. In order to investigate the sensitivity of the titanium alloy to the specimen size, the Authors carried out fatigue tests on dog-bone samples of 3.25, 4.90, and 7.30 mm in diameter, with traditional MTS testing machine under fully reversed,  $R = -1$ , force control

conditions, up to  $10^7$  cycles. The fatigue limit decreases with the specimen size, as shown in Fig. 14. In order to perform the best-fitting with Eq.(16), the experimental values of the fatigue limit can be plotted versus the specimen size in a bi-logarithmic diagram, which provides:

$$\log \Delta\sigma_{fl} = -0.41 \log b + 2.85 \quad (23)$$

It is interesting to note that a rather high value of the fractal decrement  $d_\sigma$  is obtained, which is consistent with the augmented disorder of the microstructure of the considered material. In fact, according to Li et al. [54], AM titanium alloys are characterised by a high quantity of internal defects in the form of porosity and lack of fusion defects containing un-melted particles. Fatemi et al. [55] reported that the additive manufactured (AM) samples contained many circular pores, with dimensions ranging from 5 to 80  $\mu\text{m}$ , and irregularly shaped voids with size of up to 500  $\mu\text{m}$  due to the lack of fusion [56]. As a consequence, AM can significantly reduce the fatigue strength of components [57]. Anyway, a dimensional decrement  $d_\sigma$  equal to 0.41 is less than the maximum theoretical allowed value of 0.50.

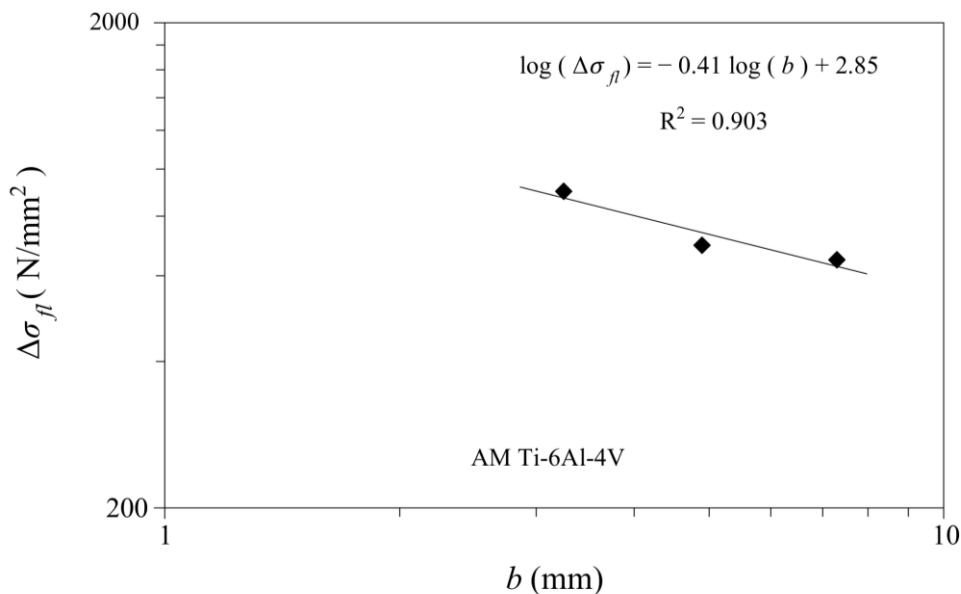


Figure 14: Experimental assessment of fatigue limit for AM Ti-6Al-4V [53]

Eventually, the experimental data set obtained by Kelly et al. [58] are analysed. In this experimental campaign, rotating bending fatigue tests were carried out on two sets of mild steel dog-bone specimens, covering a size range from 1.27 to 40.64 mm. The fitting with the MFSL of Eq.(24) provides the asymptotic value of the fatigue limit,  $\Delta\sigma_{fl}^{\infty}$ , and the material characteristic length of the material,  $l_{ch}$  (see Fig. 15). It is worth noting that the MFSL for the fatigue limit can properly interpolate the results obtained from a much wider scale range, and that very high cycle fatigue test results could be obtained as well.

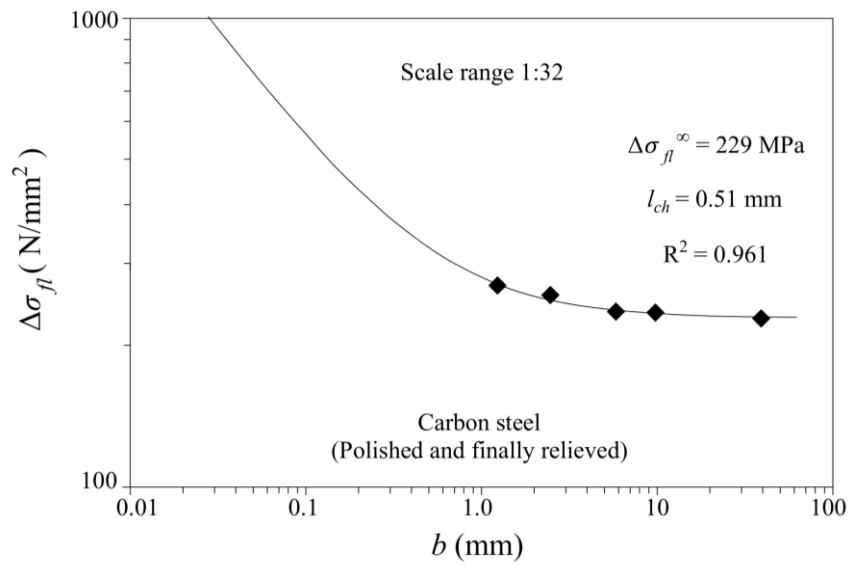


Figure 15: MFSL experimental assessment of the fatigue limit for a carbon steel (polished and finally relieved) [58]

## 6 Conclusions

When stress-life (S-N) approach was introduced in the nineteenth century, size effects were not yet known. In fact, the role of specimen size on the fatigue behaviour has been investigated only in recent times and many efforts have been made to interpret the phenomenon, which have led to the use of empirical relationships, such as the  $\sqrt{area}$  model proposed by Murakami or other statistical approaches.

In this paper, dimensional analysis and intermediate asymptotics are used to find a generalized

formulation for Wöhler's curve. Furthermore, by proposing a model based on the concept of lacunar fractality, the specimen-size dependence of Wöhler's curve is explained. The proposed models were compared to experimental data available in the Literature from which it follows that the fractal approach is able to explain the size effects on Wöhler's curve. Eventually, with the aim to provide a more accurate modelling, a multi-fractal approach is put forward both for fatigue limit and critical stress range.

### **Acknowledgments**

This research did not receive any specific grant from funding agencies in the public, commercial, or not-for-profit sectors.

### **References**

- [1] Wöhler A. Über die Festigkeitsversuche mit Eisen und Stahl. *Zeitschrift für Bauwesen*. 1870; 20: 73-106.
- [2] Basquin OH. The exponential law of endurance tests. *ASTM Proceedings*. 1910; 10: 625-630.
- [3] Schijve J. *Fatigue of Structures and Materials*. New York: Springer; 2009.
- [4] Moore RH, Harter HL. A survey of the literature on the size effect on material strength. *Journal of the American Statistical Association*. 1978; 72: 446.
- [5] Weibull W. A statistical theory for the strength of materials. *Royal Swedish Institute of Engineering Research (Ingeniörsvetenskaps Akademiens Handlingar)*. 1939; 151: 1-45.
- [6] Barenblatt GI, Botvina LR. Incomplete self-similarity of fatigue in the linear range of crack growth. *Fatigue & Fracture of Engineering Materials & Structures*. 1980; 3: 193-202.
- [7] Murakami Y. *Metal Fatigue: Effects of Small Defects and Nonmetallic Inclusions*. Oxford:

Elsiever Science; 2002.

- [8] Murakami Y, Kodama S, Konuma S. Quantitative evaluation of effects of non-metallic inclusions on fatigue strength of high strength steels. I: Basic fatigue mechanism and evaluation of correlation between the fatigue fracture stress and the size and location of non-metallic inclusions. *International Journal of Fatigue*. 1989; 11: 291-298.
- [9] Murakami Y, Usuki H. Quantitative evaluation of effects of non-metallic inclusions on fatigue strength of high strength steels. II: Fatigue limit evaluation based on statistics for extreme values of inclusion size. *International Journal of Fatigue*. 1989; 11: 299-307.
- [10] Weibull W. A Statistical Representation of Fatigue Failures in Solids. *Transactions of the Royal Institute of Technology*. 1949; 27: 1-49.
- [11] Murakami Y, Yokoyama NN, Nagata J. Mechanism of fatigue failure in ultralong life regime. *Fatigue & Fracture Engineering Materials & Structures*. 2002; 25: 735-746.
- [12] Chapetti MD, Tagawa T, Miyata T. Ultra-long cycle fatigue of high-strength carbon steels part I: Review and analysis of the mechanism of failure. *Materials Science and Engineering A*. 2003; 356: 227-235.
- [13] Bathias C, Paris P. *Gigacycle fatigue in mechanical practise*. New York: CRC Press; 2004.
- [14] Zettl B, Mayer H, Stanzl-Tschegg SE, Degischer HP. Fatigue properties of aluminium foams at high numbers of cycles. *Materials Science and Engineering A*. 2000; 292: 1-7.
- [15] Furuya Y. Notable size effects on very high cycle fatigue properties of high-strength steel. *Materials Science and Engineering A*. 2011; 528: 5234-5240.
- [16] Tridello A, Paolino DS, Chiandussi G, Rossetto M. VHCF response of AISI H13 steel: Assessment of size effects through Gaussian specimens. *Procedia Engineering*. 2015; 109: 121-127.
- [17] Tridello A, Paolino DS, Chiandussi G, Rossetto M. Different inclusion contents in H13 steel: Effects on VHCF response of Gaussian specimen. *Key Engineering Materials*. 2016; 665: 49-52.
- [18] Tridello A, Paolino DS, Chiandussi G, Rossetto M. Comparison between dog-bone and Gaussian specimens for size effect evaluation in gigacycle fatigue. *Frattura e Integrità Strutturale*. 2013; 26: 49-56.

- [19] Paolino DS, Tridello A, Chiandussi G, Rossetto M. On specimen design for size effect evaluation in ultrasonic gigacycle fatigue testing. *Fatigue & Fracture of Engineering Materials & Structures*. 2014; 37: 570-579.
- [20] Tridello A, Paolino DS, Chiandussi G, Rossetto M. VHCF strength decrement in large H13 steel specimens subjected to ESR process. *Procedia Structural Integrity*. 2016; 2: 1117-1124.
- [21] Carpinteri A. Scaling laws and renormalization groups for strength and toughness of disordered materials. *International Journal of Solids and Structures*. 1994; 31: 291-302.
- [22] Carpinteri A, Spagnoli A, Vantadori S. Size effect in S-N curves: A fractal approach to finite-life fatigue strength. *International Journal of Fatigue*. 2009; 31: 927-933.
- [23] Carpinteri A, Paggi M. A unified interpretation of the power laws in fatigue and the analytical correlations between cyclic properties of engineering materials. *International Journal of Fatigue*. 2009; 31: 1524-1531.
- [24] Carpinteri A, Paggi M. Dimensional analysis and fractal modeling of fatigue crack growth. *Journal of ASTM International*. 2011; 8: 1-13.
- [25] Buckingham E. Model experiment and the form of empirical equation. *ASME Transaction*. 1915; 37: 263-296.
- [26] Carpinteri A. Notch sensitivity in fracture testing of aggregative materials. *Engineering Fracture Mechanics*. 1982; 16: 467-481.
- [27] Barenblatt GI. *Scaling, Self-similarity and Intermediate Asymptotics*. UK: Cambridge University Press; 1996.
- [28] Barenblatt GI. *Scaling*. UK: Cambridge University Press; 2003.
- [29] Barenblatt G.I. Scaling Phenomena in Fatigue and Fracture. *International Journal of Fracture*. 2006; 138: 19-35.
- [30] Carpinteri A, Montagnoli F. Scaling and fractality in subcritical fatigue crack growth: Crack-size effects on Paris' law and fatigue threshold. *Fatigue & Fracture of Engineering Materials & Structures*. 2020; 43: 788-801.
- [31] Falconer K. *Fractal Geometry: Mathematical Foundations and Applications* Chichester: Wiley; 1990.

- [32] Carpinteri A. Fractal nature of material microstructure and size effects on apparent mechanical properties. *Mechanics of Materials*. 1994; 18: 89-101. Internal Report, Laboratory of Fracture Mechanics, Politecnico di Torino, N. 1/92, 1992.
- [33] Carpinteri A, Ferro G. Size effects on tensile fracture properties: a unified explanation based on disorder and fractality of concrete microstructure. *Materials and Structures (RILEM)*. 1994; 27: 563-571.
- [34] Carpinteri A, Chiaia B. Power scaling laws and dimensional transitions in solid mechanics. *Chaos, Solitons & Fractals*. 1996; 7: 1343-1364.
- [35] Carpinteri A, Chiaia B. Fractals, Renormalization group theory and scaling laws for strength and toughness of disordered materials. In: Breysse D, ed. *Proceedings of the workshop probabilities and materials: tests, models and applications*. Cachan, France: Kluwer Acad Publishers; 1994: 141-150.
- [36] Carpinteri A, Chiaia B. Multifractal scaling laws in the scaling behaviour of disordered materials. *Chaos, Solitons & Fractals*. 1997; 8: 135-150.
- [37] Carpinteri A, Chiaia B, Ferro G. Size effects on nominal tensile strength of concrete structures: multifractality of material ligaments and dimensional transition from order to disorder. *Materials and Structures*. 1995; 28: 311-317.
- [38] Carpinteri A, Ferro G, Invernizzi S. The nominal tensile strength of disordered materials: A statistical fracture mechanics approach. *Engineering Fracture Mechanics*. 1997; 58: 421-435.
- [39] Carpinteri A, Chiaia B, Cornetti P. On the mechanics of quasi-brittle materials with a fractal microstructure. *Engineering Fracture Mechanics*. 2003; 70: 2321-2349.
- [40] Carpinteri A, Chiaia B, Cornetti P. A scale-invariant cohesive crack model for quasi-brittle materials. *Engineering Fracture Mechanics*. 2002; 69: 207-217.
- [41] Carpinteri A, Cornetti P, Puzzi S. Scaling laws and multiscale approach in the mechanics of heterogeneous and disordered materials. *Applied Mechanics Reviews*. 2006; 59: 283-305.
- [42] Carpinteri A, Chiaia B, Ferro G. A new explanation for size effects on the flexural strength of concrete. *Magazine of Concrete Research*. 1997; 49: 45-53.
- [43] Carpinteri A, Chiaia B, Ferro G. Scale dependence of tensile strength of concrete specimens: A multifractal approach. *Magazine of Concrete Research*. 1998; 50: 237-246.

- [44] Carpinteri A, Chiaia B. Multifractal nature of concrete fracture surfaces and size effects on nominal fracture energy. *Materials and Structures*. 1995; 28: 435-443.
- [45] Carpinteri A, Spagnoli A, Vantadori S. An approach to size effect in fatigue of metals using fractal theories. *Fatigue & Fracture Engineering Materials & Structures*. 2002; 25: 619-627.
- [46] Montagnoli F, Invernizzi S, Carpinteri A. Fractality and size effect in fatigue damage accumulation: Comparison between Paris and Wöhler perspectives. *Lecture Notes in Mechanical Engineering*. 2020 (In print).
- [47] Tomaszewsky T, Sempruch J. Analysis of size effect in high-cycle fatigue for EN AW-6063. *Solid State Phenomena*. 2015; 224: 75-80.
- [48] Xue H, Sun Z, Zhang X, Gao T, Li Z. Very high cycle fatigue of cast aluminium alloy: Size effect and crack initiation. *Journal of Materials Engineering and Performance*. 2018; 27: 5406-5416.
- [49] Hatanaka K, Shimizu S, Nagae A. Size effect on rotating bending fatigue in steels. *Bulletin of the JSME*. 1983; 26: 1288-1295.
- [50] Carpinteri A, Montagnoli F. Scaling and fractality in fatigue crack growth: Implications to Paris' law and Wöhler's curve. *Procedia Structural Integrity*. 2019; 14: 957-963.
- [51] Carpinteri A. *Mechanical Damage and Crack Growth in Concrete: Plastic collapse to brittle fracture*. New York: John Wiley & Sons; 1986.
- [52] Furuya Y. Size effects in gigacycle fatigue of high-strength steel under ultrasonic fatigue testing. *Procedia Engineering*. 2010; 2: 485-490.
- [53] Pegues J, Roach M, Williamson RS, Shamsaei N. Volume effects on the fatigue behavior of additively manufactured Ti-6Al-4V Parts. In: Bourell DL, Beaman JJ, Crawford RH, Fish S, Seepersad FS, eds. *Proceedings of the 29<sup>th</sup> Annual International Solid Freeform Fabrication Symposium – An additive Manufacturing Conference*. Austin, USA: University of Texas at Austin; 2018: 1373-1381.
- [54] Li P, Warner D, Fatemi A, Phan N. Critical assessment of the fatigue performance of additively manufacturing Ti-6Al-4V and perspective for future research. *International Journal of Fatigue*. 2016; 85: 130-143.
- [55] Fatemi A, Molaei R, Sharifimehr S, Phan N, Shamsaei N. Multiaxial fatigue behavior of wrought

and additive manufactured Ti-6Al-4V including surface finish effect. *International Journal of Fatigue* 2017; 100: 347-366.

[56] Fatemi A, Molaei R, Sharifimehr S, Shamsaei N, Phan N. Torsional fatigue behavior of wrought and additive manufactured Ti-6Al-4V by powder bed fusion including surface finish effect. *International Journal of Fatigue* 2017; 99: 187-201.

[57] Fatemi A, Molaei R, Simsiriwong J, Sanaei N, Pegues J, Torries B, Phan N, Shamsaei N. Fatigue behaviour of additive manufactured materials: An overview of some recent experimental studies on Ti-6Al-4V considering various processing and loading direction effects. *Fatigue & Fracture of Engineering Materials & Structures*. 2019; 42: 991-1009.

[58] Kelly DA, Morrison JLM. Effect of specimen size and preparation on the fatigue strength of a plain carbon steel tested in rotating bending and in torsion. *Proceedings of the Institution of Mechanical Engineers* 1970; 185: 655-664.